

Towards the next step: SpaceLiner 8 pre-definition

Martin Sippel, Jascha Wilken, Steffen Callsen, Leonid Bussler

Martin.Sippel@dlr.de Tel. +49-421-244201145

DLR Space Launcher System Analysis (SART), Bremen, Germany

The SpaceLiner fully reusable launcher and ultra-high-speed rocket-propelled passenger transport is in conceptual design phase. The ongoing concept evolution is addressing system aspects of the next configuration release 8. The winged, reusable upper stage, almost untouched since 2016 is moving now in focus of promising redesign options described in this paper.

The SpaceLiner cabin integration is an important aspect to be addressed as well as the feasibility of performing multiple missions compliant with noise and sonic-boom constraints. The systematic assessment of different critical separation cases revealed that the aerodynamic unstable design of the capsule is not acceptable and needs to be redesigned for SpaceLiner 8. Further, the nose section of a future SLC should include part of the separation motors and thus help improving stability of the emergency-case separation maneuvers.

Keywords: RLV, LOX-LH2-propulsion, SpaceLiner, point-to-point passenger transport

Nomenclature

D	Drag	N
I_{sp}	(mass) specific Impulse	s (N s / kg)
L	Lift	N
M	Mach-number	-
T	Thrust	N
W	Weight	N
g	gravity acceleration	m/s ²
m	mass	kg
q	dynamic pressure	Pa
v	velocity	m/s
α	angle of attack	-
γ	flight path angle	-

TVC	Thrust Vector Control
CoG	center of gravity
cop	center of pressure

1 INTRODUCTION

The key premise behind the original concept inception is that the SpaceLiner ultimately has the potential to enable sustainable low-cost space transportation to orbit while at the same time revolutionizing ultra-long-distance travel between different points on Earth. The number of rocket launches per year should be strongly raised and hence manufacturing and operating cost of launcher hardware should dramatically shrink.

DLR's SpaceLiner concept is similar in certain aspects to the idea of multiple-mission reusable launch vehicles. These concepts are understood to serve quite diverse missions by the same or at least a similar vehicle. Another typical example in this category is the SpaceX Starship&SuperHeavy (formerly called BFR) [1, 2]. While in its primary role conceived as an ultrafast intercontinental passenger transport, in its second role the SpaceLiner is intended as an RLV capable of delivering heavy payloads into orbit. Currently available, simulations proof that the SpaceLiner orbital version stays within the load constraints of the PAX-version which confirms feasibility of the multiple mission intention.

First proposed in 2005 [3], the SpaceLiner is under constant development and descriptions of some major updates have been published since then [4, 8 - 11, 17, 18]. The European Union's 7th Research Framework Programme has supported several important aspects of multidisciplinary and multinational cooperation in the projects FAST20XX, CHATT, HIKARI, and HYPMOCES. In the EU's Horizon 2020 program the project FALCon addressed the advanced return recovery mode "in-air-capturing" to be used by the reusable booster stage [21, 22, 23]. The way how such hypersonic point-to-point transports like SpaceLiner are to be integrated in future controlled airspace was addressed in the SESAR-project ECHO. The SpaceLiner has been one of the reference concepts and feasible intercontinental trajectories are refined in DLR-SART analyses [24, 24].

An important milestone was reached in 2016 with the successful completion of the Mission Requirements Review (MRR) which allows the concept to mature from research to

Subscripts, Abbreviations

AOA	Angle of Attack
ATM	Air Traffic Management
CAD	Computer Aided Design
CFD	Computational Fluid Dynamics
CMC	Ceramic Matrix Composites
CRS	Cabin Rescue System
DOF	Degree of Freedom
GLOW	Gross Lift-Off Mass
LEO	Low Earth Orbit
LH2	Liquid Hydrogen
LOX	Liquid Oxygen
MECO	Main Engine Cut Off
MR	mixture ratio
MRR	Mission Requirements Review
NPSP	Net Positive Suction Pressure
OTP	Oxidizer Turbo Pump
PEEK	Poly-ether-ether ketone
RCS	Reaction Control System
RLV	Reusable Launch Vehicle
SLB	SpaceLiner Booster stage
SLC	SpaceLiner Cabin
SLME	SpaceLiner Main Engine
SLO	SpaceLiner Orbiter stage
SLP	SpaceLiner Passenger stage
TAEM	Terminal Area Energy Management
TPS	Thermal Protection System
TRL	Technology Readiness Level
TSTO	Two-Stage-To-Orbit

structured development [17]. The Mission Requirements Document (MRD) [7] is the baseline and starting point for all technical and programmatic follow-on activities of the SpaceLiner Program.



Figure 1: Rendering of SpaceLiner 7-3 upper stage in high altitude gliding flight over Alaska

2 SPACELINER 7 ARCHITECTURE, GEOMETRY AND MAIN COMPONENTS

The current arrangement of the two SpaceLiner stages, the reusable booster and the orbiter or passenger stage, at lift-off is presented in Figure 2. All LOX-feedlines and the LH₂-crossfeed connection are attached on the booster's top outer side, thus, subjected to flow in the relatively cold wake region. The feedlines of the upper stage are completely internal and ducted underneath the TPS. An adapted feedline and crossfeed system is needed for the LOX-tank of the TSTO orbiter stage bypassing the satellite cargo-bay (Figure 2, top).

The main dimensions of the 7-3 booster configuration are listed in Table 1 while major geometry data of the SpaceLiner 7-3 passenger or orbiter stage are summarized in Table 2.

Table 1: Geometrical data of SpaceLiner 7-3 booster stage (SLB)

length [m]	span [m]	height [m]	fuselage diameter [m]	wing leading edge angles [deg]	wing pitch angle [deg]	wing dihedral angle [deg]
82.3	36.0	8.7	8.6	82/61/43	3.5	0

Table 2: Geometrical data of SpaceLiner 7-3 passenger / orbiter stage (SLP / SLO)

length [m]	span [m]	height [m]	fuselage diameter [m]	wing leading edge angle [deg]	wing pitch angle [deg]	wing dihedral angle [deg]
65.6	33.0	12.1	6.4	70	0.4	2.65

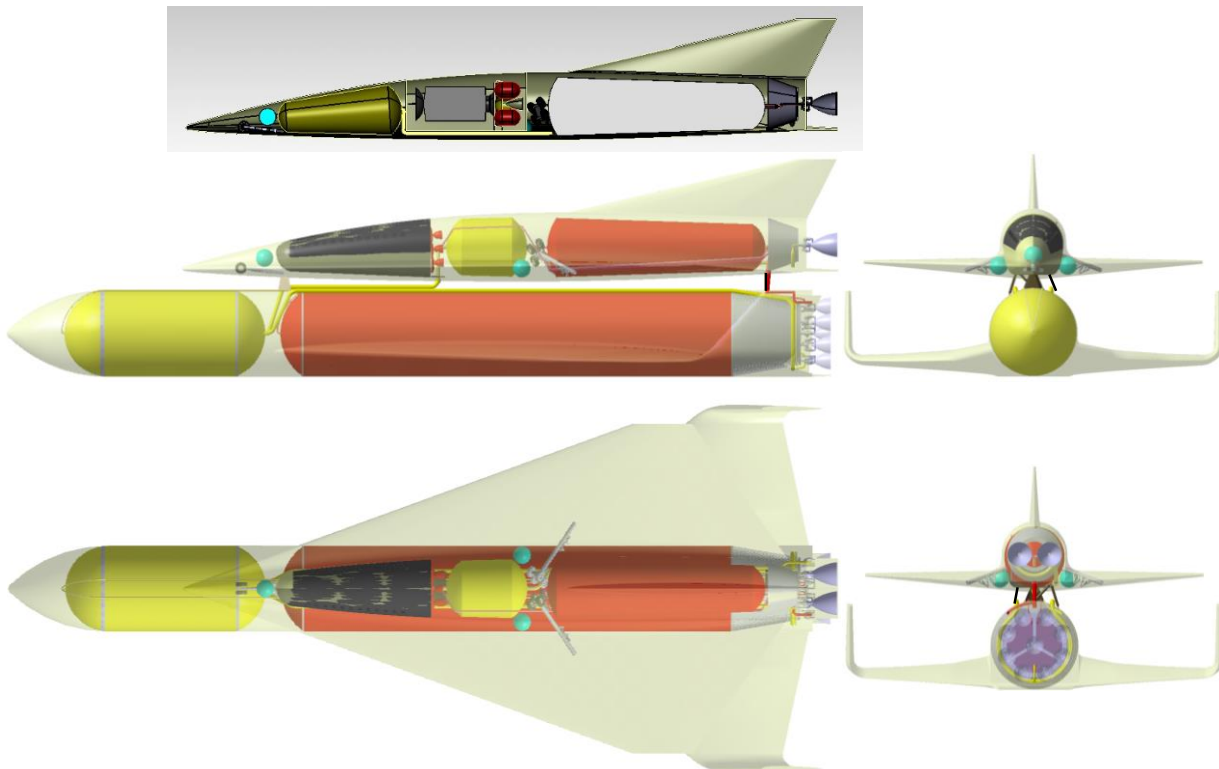


Figure 2: Sketch of SpaceLiner 7-3 launch configuration with passenger version (SLP) with its booster stage at bottom position and orbital stage of SLO in insert at top

2.1 Main propulsion system

Staged combustion cycle rocket engines with a moderate 16 MPa chamber pressure have been selected as the baseline propulsion system right at the beginning of the project [3]. A Full-Flow Staged Combustion Cycle with a fuel-rich

preburner gas turbine driving the LH₂-pump and an oxidizer-rich preburner gas turbine driving the LOX-pump is the preferred design solution for the SpaceLiner Main Engine (SLME). It is interesting to note that the ambitious full-flow cycle is currently developed by SpaceX for its Starship&-SuperHeavy with the Raptor-engine [37]. This concept is in

some aspects a similar multiple mission reusable launch vehicle as SpaceLiner intends to become [10]. The Raptor engine is influenced by its interplanetary mission and hence is using a different propellant combination LOX-LCH4 which might one day be produced in-situ on Mars.

The expansion ratios of the booster and passenger stage / orbiter SLME engines are adapted to their respective optimums; while the mass flow, turbo-machinery, and combustion chamber are assumed to remain identical in the baseline configuration [19].

The SpaceLiner 7 has the requirement of vacuum thrust up to 2350 kN and sea-level thrust of 2100 kN for the booster engine and 2400 kN, 2000 kN respectively for the passenger stage. All these values are given at a mixture ratio of 6.5 with a nominal operational MR-range requirement from 6.5 to 5.5. The full pre-defined operational domain of the SLME is shown in [20] including extreme operating points. Table 3 gives an overview about major SLME engine operation data for the nominal MR-range as obtained by latest cycle analyses [20]. Performance data are presented for the two different nozzle expansion ratios of the SpaceLiner: 33 and 59.

Subcomponent sizing and definition is progressing at Phase A conceptual design level. Refinements are focusing on the turbomachinery designed as an integrated power-head and a suitable regeneratively cooled thrust-chamber lay-out. An Integrated Power Head (Pre-burner + Turbine + Impeller pump) as it has been used on the SSME is also the preferred design solution for the SLME. The reduced length of high-pressure hot gas lines should enable significant mass saving and a compact and clean lay-out [19, 20]. Both preburners' external walls are actively cooled by their respective predominant fluids. The cooling fluid is heated up and subsequently used as pressurization gas for the tanks [19]. In order to preliminarily understand the combustion and flow interactions, CFD simulations with a very simplified, preliminary 2D geometry of a potential SLME preburner were carried out [20]. The commercial CFD solver ANSYS CFX was used for the first series of numerical analyses.

The commercial AxSTREAM® software tool for turbomachinery analyses has been implemented. AxSTREAM® is a multidisciplinary design, analysis and optimization software platform that provides fully integrated and streamlined solutions, encompassing the complete turbomachinery design process, all in a seamless interactive user interface. The following turbomachinery components have been pre-designed: LPFTP pump and turbine, HPFTP pump and turbine

and HPOTP pump and turbine. The thermodynamic parameters used for the turbomachines design correspond to the demanding operational point O2 and the SLME cycle design conditions of 2019, mostly similar to those presented in [19]. Consolidated size, mass, and performance data are available by this analysis and are integrated in the engine model.

Figure 3 shows the integration of all major components of the Integrated Power Head in the upper section of the SLME and their integration with the combustion chamber injector head. The preliminary layout from [17, 19] is maintained but in this consolidated design also considering the preliminary sizing of the regenerative cooling and of the turbopumps.

The size of the SLME in the smaller booster type is a maximum diameter of 1800 mm and overall length of 2981 mm. The larger second stage SLME has a maximum diameter of 2370 mm and overall length of 3893 mm. Both engine variants are shown with their Integrated Power Head architecture of turbo-machinery and two preburners as simplified CAD-models in Figure 3.

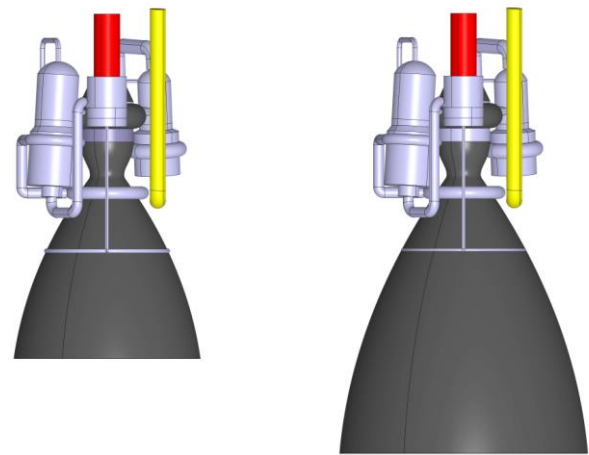


Figure 3: SLME simplified CAD geometry with nozzle expansion ratio 33 (left) and 59 (right) [20]

The engine masses are estimated at 3375 kg with the large nozzle for the upper stage and at 3096 kg for the booster stage. These values are equivalent to vacuum T/W at MR=6.0 of 68.5 and 72.6 [20].

Currently, the Swiss company SoftInway and DLR jointly perform a de-risk study for ESA on the SLME-type rocket engine.

Table 3: SpaceLiner Main Engine (SLME) technical data from numerical cycle analysis [20]

Operation point	O1	O1	O2	O2	O3	O3
Mixture ratio [-]	6		6.5		5.5	
Chamber pressure [MPa]	16		16.95		15.1	
Mass flow rate in MCC [kg/s]	513.5		555		477.65	
Expansion ratio [-]	33	59	33	59	33	59
Specific impulse in vacuum [s]	436.9	448.95	433.39	445.97	439	450.56
Specific impulse at sea level [s]	385.9	357.77	386.13	361.5	384.2	352.6
Thrust in vacuum per engine [kN]	2200	2260.68	2358.8	2427.28	2056.7	2110.49
Thrust at sea level per engine [kN]	1943	1801.55	2101.6	1967.32	1800	1651.56

2.2 Reusable booster stage

The SpaceLiner 7 booster geometry is relatively conventional with two large integral tanks with separate bulkheads for LOX and LH2 which resembles the Space Shuttle External tank

(ET) lay-out [9]. The major additions to the ET are an ogive nose for aerodynamic reasons and for housing subsystems, the propulsion system, and the wing structure with landing gear. The two tanks are part of the load carrying structure. The structure of the wing follows aircraft convention with ribs to

make up the shape of the wing profile and spars to carry the main bending load [18]. Both tanks with an external structural diameter of 8.5 m carry all major loads. The interface thrust to the upper stage is going through the intertank structure right in front of the very large LH2 tank with a total internal volume of 2577 m³. Engine thrust and the ground support loads at the launch pad are directed through the conical thrust frame which is connected to the aft-Y-ring of the hydrogen tank. The baseline structural design utilizes integrally stringer/frame stiffened aluminum lithium (Al-Li) 2195 skins for the “fuselage” (LOX & LH2 tanks, nose cone, inter-tank-structure, aft skirt), and 2195 honeycomb sandwich panels for the wings. The current configuration of the booster has been defined based on extensive analyses of the propellant crossfeed system [19, 20].

The booster wing (and winglet) airfoils have been selected as modified NPL-EC/ECH cut at trailing edge thickness of 75 mm [12]. The relative backward position of maximum chord thickness is beneficial for drag reduction in the supersonic and hypersonic flow (thus improved L/D) and at the same time allows for good structural efficiency where the largest aerodynamic lift forces are introduced.

Return to the launch site of the SLB is traditionally assumed to make use of the patented “in-air-capturing”-method which likely provides the best performance [21, 22]. Full simulations of the SLB-recovery are still open and should be performed in the future for the SLB8-configuration.

2.3 Reusable upper stage

The SpaceLiner7 aerodynamic shape is a result of a trade-off between the optima fulfilling the requirements of three reference trajectory points. Numerical analyses have pointed out the clear advantages of a single delta wing [12, 13]. Major geometry data of the SpaceLiner 7-3 passenger and orbiter stage are summarized in Table 2. The SpaceLiner passenger stage’s shape is shown in Figure 4.



Figure 4: SpaceLiner 7-3 passenger stage

The SpaceLiner 7 passenger stage achieves without flap deflection an excellent hypersonic L/D of 3.5 up to M=14 assuming a fully turbulent boundary layer. The laminar-turbulent transition is assumed occurring at an altitude of 58 km which is around Mach 18 [12].

In some areas of the SpaceLiner passenger stage (leading edge and nose) the heatflux and temperatures exceed those values acceptable by CMC used in the passive TPS [8, 17]. Already early in the project, transpiration cooling using liquid water has been foreseen as a potential option for solving the problem [4, 14]. In the EU-funded project FAST20XX this innovative method has been experimentally tested in DLR’s arc heated facility in Cologne using subscale probes of different porous ceramic materials [15]. Test results have been scaled to full-size by heat transfer correlations and numerical assessment of the complete SpaceLiner trajectory [14]. Based on these data,

a water storage tank system, a feedline manifold including control and check-valves and some bypass and redundancy lines were preliminarily sized for accommodation inside the SpaceLiner volume for which an early mass estimation was obtained [16].

Besides the overall promising results also some technical challenges of the active transpiration cooling system have been detected in the FAST20XX-investigations. Precise controllability of the water flow through the porous ceramic media has been found difficult. The experiments sometimes were running into over or under supply of water which could not be recovered within the same experimental run. A more sophisticated supply system would be needed in a flight vehicle. Another concern is the fact that the gas flow from the coolant might trigger early boundary-layer transition. As a consequence, some areas of the passive TPS might need to be reinforced. Therefore, the active transpiration cooling of leading edges and nose is still the reference design option but could once be replaced by other means of active cooling [16].

The passenger stage’s internal design has been adapted for its secondary role as an unmanned satellite launcher. The passenger cabin (see separate section 2.4 below!) is not needed for this variant and is instead replaced by a large internal payload bay [17]. Key geometrical constraints and requirements are set that the SpaceLiner 7 passenger stage’s outer mold line and aerodynamic configuration including all flaps should be kept unchanged. The internal arrangement of the vehicle could be adapted; however, maximum commonality of internal components (e.g. structure, tanks, gear position, propulsion and feed system) to the passenger version is preferred because of cost reflections.

Further, the payload bay should provide sufficient volume for the accommodation of a large satellite and its orbital transfer stage [9]. For this purpose, the stage’s propellant loading has been reduced by 24 Mg to 190 Mg with a smaller LOX-tank to allow for a payload bay length of 12.1 m and at least 4.75 m diameter [17]. These dimensions are close to the Space Shuttle (18.3 m x 5.18 m x 3.96 m) and should accommodate even super-heavy GTO satellites of more than 8 m in length and their respective storable upper stage. Large doors open on the upper side to enable easy and fast release of the satellite payload in orbit.

The orbiter stage mass has been estimated based on the SpaceLiner 7-3 passenger stage budget (see Table 5 on p. 6). Adaptations include the complete removal of all cabin related masses. Instead a mass provision for the payload bay and its mechanisms including doors, the mounting structure, and also a radiator system for on-orbit heat-control is added. The resulting orbiter dry mass is about 102 Mg and the budget is listed in Table 6.

The aerodynamic trimming of the satellite transport stage with the existing trailing edge flaps and the bodyflap has been preliminarily checked in numerical simulation under hypersonic flow conditions of atmospheric reentry and is found feasible within the constraints of the 7-3 lay-out [17]. This promising outcome is a result of the robust SpaceLiner design philosophy which is also taking into account off-nominal abort flights. The calculated maximum L/D is reduced approximately 15% by the significant flap deflections compared to the L/D achievable for the nominal passenger mission with almost no deflection. Nevertheless, the once-around-Earth-mission of the orbiter is not compromised as demonstrated by reentry trajectory simulations [17].

2.4 SpaceLiner Cabin and Rescue System

The passenger cabin of the SpaceLiner has a double role. Providing first a comfortable pressurized travel compartment which allows for horizontal entrance of the passengers, the cabin in its second role serves as a reliable rescue system in case of catastrophic events. Thus, the primary requirements of the cabin are the possibility of being firmly attached late in the launch preparation process and fast and safely separated in case of an emergency.

The capsule should be able to fly autonomously back to Earth's surface in all separation cases. The abort trajectories are primarily influenced by the mass of the capsule and the aerodynamic performance with the most important subsystems being the separation motors, the thermal protection system (TPS), and the structure.

The SpaceLiner MRD [7, 17] defines passenger safety requirements well beyond today's reliability of launch vehicles which are nevertheless indispensable to create a viable commercial product. A safety philosophy following a multiple step approach is chosen to address the MRD-requirement:

- built-in safety and redundancy with continuous monitoring of flight critical functions and if necessary early shut-down of systems to avoid catastrophic events,
- engine-out capability during the full mission including vehicle controllability in adverse conditions [28],
- capability of the passenger stage SLP to perform abort flight maneuvers in case an early separation from the booster stage would be required during ascent,
- in case of extreme emergencies in which the previously listed safety measures are not sufficient to save life on board or can't be used anymore, the SLC will be separated and rapidly distance itself from a launch vehicle no longer controllable. Only this special case of SLC separation and its subsequent free flight conditions are relevant for the study results of this section.

Overall length of the capsule for 50 passengers (without separation motors) is 15.6 m and its maximum external height is 5.6 m. The estimated masses of the capsule are about 25.5 tons for the dry capsule, about 7600 kg for the passengers, crew and luggage, and 3800 kg for all propellants, separation motor, retro-rockets and RCS [18].

The capsule can be subdivided in a pressurized cabin of conical shape and an outer aerodynamic shell formed by the Thermal Protection System and which provides space for housing several non-pressurized subsystems [8, 17, 31]. The TPS of the SpaceLiner7 capsule is required to withstand several different heat load conditions driven by the different nominal and abort cases it might encounter. During nominal flight the capsule in its baseline design is considered to have its upper part conformal with the topside of the passenger stage (SLP). The SLC lower section is clamped within the SLP without any load carrying structural connection (see e.g. [18]) to allow rapid and safe separation in case of an emergency.

The separation motors attached to the rear end of the SpaceLiner Capsule (SLC) are of crucial importance for the capsule ejection procedure. Due to severe geometry constraints, it has been decided early to utilize a five-motor configuration with very short cylindrical section. By the use of innovative multi-nozzle motors, expansion ratio could reach $\varepsilon = 21$. The maximum thrust with a chamber pressure of 15 MPa is around 856 kN at sea-level ($I_{sp} = 267$ s) and 908 kN ($I_{sp} = 290$ s) in vacuum. The total mass per motor is approxi-

mately 693 kg leading to a total mass for all motors of 3.47 tons [43, 44].

A preliminary design for the capsule's main subsystems has been elaborated [18, 29] including the body flaps, deployable rudders, the parachute system for transonic stabilization and landing, the electro-mechanical actuators and their batteries, and the reaction control system (RCS). A double bodyflap and two deployable control fins on the upper surface support flight controllability and stability. The RCS choice is characterized by 2 clusters of thrusters located in the rear part of the capsule. Each cluster provides a thrust of 3 kN along each of the double axis for a total delivered thrust of 12 kN. Parachutes are assumed to be deployed and operate in a certain altitude-Mach-box to decelerate the capsule during the final landing phase. The SpaceLiner capsule parachute system is likely a combination of supersonic stabilization chute which allows safe deceleration through the transonics and subsequent subsonic gliding by parafoil [18, 29].

Multi-body 6DOF-simulations using Simpack have been set up for the analyses of the baseline SLC integration as shown in Figure 5 [43, 44]. Five abort cases with SLC ejection along the nominal operational flight have been analyzed with multi-body simulations. Initial conditions are used in all cases from the nominal passenger flight trajectory without assuming any degradation in flight path or attitude due to anomalies. Obviously, this is a major simplification of potential emergency situations and is not reflecting a worst-case scenario. However, the analyses presented in [43, 44] intended to use these trade-offs to serve in the definition of system requirements in the Phase A analyses.

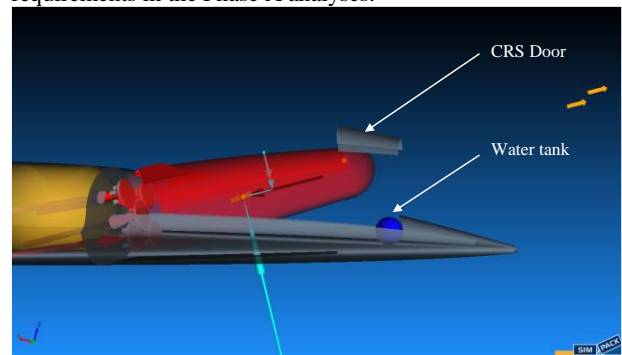


Figure 5: Simulation of SLC7 early in separation phase [42]

References 43 and 44 are presenting the axial accelerations acting on seat rows in the most forward and most aft position of the SLC depending on the separation conditions of the five cases. Around 0.4 s after initiation of the process approximately 12 g are reached in axial direction with burn duration of 2 s and in case of the aft row, very short peaks even approach up to 14 g [43, 44]. With the motors burn-out the acceleration levels are sharply reduced, nevertheless, in some cases oscillating around $\pm 2g$ due to SLC rotation and the effect of aerodynamic forces. Medical investigations of NASA had demonstrated in the past that even untrained passengers will endure such elevated acceleration levels for a short time if pushed back into their seats ("eyeballs in") and somehow less in the opposite direction ("eyeballs out") corresponding here to negative n_x .

The human body is more sensitive to normal acceleration levels, pressed downward into the seats or lifted upward out of the seats, the latter corresponding to negative n_z . In case of separation at maximum dynamic pressure, the strong aerody-

dynamic forces are influencing the acceleration profile and severe oscillations with high angular accelerations have been detected due to relatively fast rotation of the capsule [42, 43, 44]. The results clearly indicate that SLC separation at maximum dynamic pressure in transonics during ascent flight is highly critical and is not safely feasible in the current aerodynamic design of SLC7.

A preliminary assessment of the results in [43, 44] revealed that the problem is relevant for the full section of SpaceLiner flight at elevated dynamic pressure. The initial approach of actively controlling by RCS-thrusters turns out to be unfeasible at elevated dynamic pressure levels. Thrusters would have to be upscaled to an excessive size and mass. Instead the SLC needs to be redesigned for SpaceLiner 8 that its shape is aerodynamically stable or could rapidly morph into

a stable configuration. Preliminary design trade-offs are discussed in section 3.4.

2.5 System masses

Based on available subsystem sizing and empirical mass estimation relationships, the stage masses have been derived as listed in Table 4 through Table 6. In case of the passenger stage (Table 5), the total fluid and propellant mass includes all ascent, residual, and RCS propellants and the water needed for the active leading edge cooling [4, 8, 16, 17]. The stages' MECO mass is approximately 151.1 Mg.

The SpaceLiner 7-3's GLOW reaches about 1832 Mg (Table 7) for the reference mission Australia – Europe while the TSTO is at 1807 Mg (Table 8) still below that of the Space Shuttle STS of more than 2000 Mg.

Table 4: Mass data of SpaceLiner 7-3 booster stage

Structure [Mg]	Propulsion [Mg]	Subsystem [Mg]	TPS [Mg]	Total dry [Mg]	Total propellant loading [Mg]	GLOW [Mg]
123.5	36.9	18.9	19.1	198.4	1272	1467

Table 5: Mass data of SpaceLiner 7-3 passenger stage

Structure [Mg]	Propulsion [Mg]	Subsystems including cabin [Mg]	TPS [Mg]	Total dry [Mg]	Total fluid & propellant loading [Mg]	GLOW incl. passengers & payload [Mg]
55.3	9.7	43.5	22.3	129	232.1	366

Table 6: Mass data of SpaceLiner 7 Orbiter stage (GTO mission)

Structure [Mg]	Propulsion [Mg]	Subsystems [Mg]	TPS [Mg]	Total dry [Mg]	Total fluid & propellant loading [Mg]	GLOW incl. kick-stage & payload [Mg]
60.1	9.9	9.8	22.3	102	207	309.1

Table 7: Mass data of SpaceLiner 7-3 passenger launch configuration

Total dry [Mg]	Total propellant loading [Mg]	GLOW incl. passengers & payload [Mg]
327.4	1502	1832.2

Table 8: Mass data of SpaceLiner 7-3 TSTO launch configuration

Total dry [Mg]	Total propellant loading [Mg]	GLOW incl. kick-stage & payload [Mg]
300.6	1467	1807

2.6 Reference trajectories

Possible SpaceLiner trajectories have been calculated since the early investigations started. The current configuration 7-3's flight path options are presented in references 2, 9, 10. Figure 6 shows some key-characteristics of the reference mission Australia to Europe. After its vertical take-off the 7-3-configuration is initially following a typical ascent profile of a rocket launcher. Succeeding the booster stage separation, the passenger stage is accelerated almost horizontally being the most energy-efficient way for a stage with good hypersonic L/D-ratio and intentionally long unpropelled gliding phase. Thus, second stage MECO is at slightly lower altitude than booster MECO. Axial acceleration is limited to 2.5 g which is achieved by engine throttling and subsequent engine shut-downs on the booster stage. The short acceleration-peak at SLP MECO exceeding this limitation is an artefact of the simplified simulation and disappears when assuming a

realistic engine shut-down sequence. Normal acceleration n_z is smoothly approaching 1 g during the gliding phase while axial deceleration is then around -0.1 g.

Launch of the SpaceLiner 7 TSTO orbital launcher has been simulated from the Kourou space center into a low 30 km × 250 km transfer orbit. Actually, this trajectory allows at least for the GTO mission that the orbiter stage becomes a once-around-Earth-vehicle capable of reaching its own launch site after a single circle around the planet. As a consequence, the achievable payload mass increases and overall complexity is reduced; e.g. an active deorbiting is not needed. Trajectory optimizations show that the orbiter is able to deliver internally more than 26150 kg of separable payload to the very low and unstable orbit.

Figure 7 shows the Mach-altitude-profile of the reusable stages for the GTO-mission. Note the overall very similar

behavior between passenger (Figure 6) and cargo reference missions of the ascent segment until booster separation.

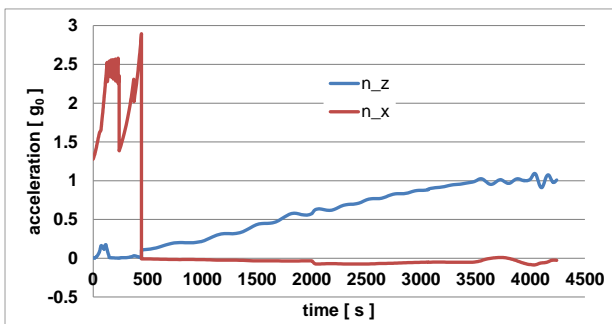
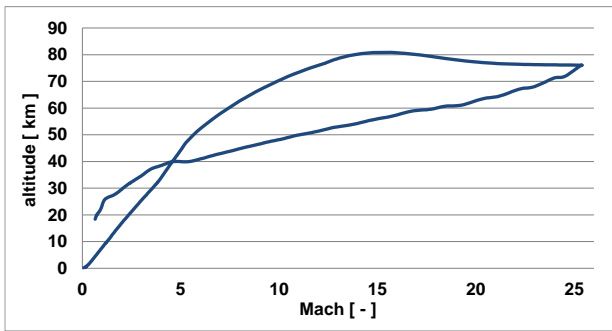


Figure 6: Calculated trajectory characteristics of SpaceLiner 7-3 reference mission Australia to Europe

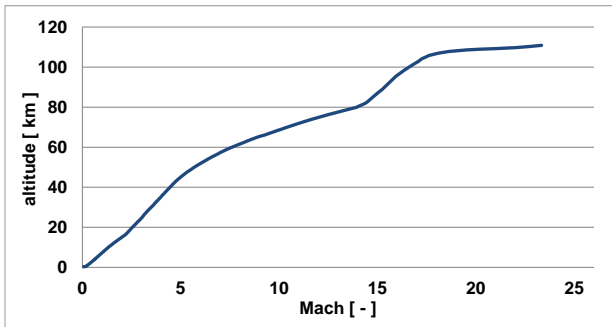


Figure 7: Calculated trajectory characteristics of SpaceLiner 7-3 orbital mission (GTO) plotted up to SLO MECO

Subsequently, an orbital transfer is necessary from LEO to GTO. A generic storable propellant upper stage has been selected for payload transfer from $30 \text{ km} \times 250 \text{ km}$ to the $250 \text{ km} \times 35786 \text{ km}$ GTO. The main reason for this choice is the restricted volume inside the payload bay which does not allow accommodating both the larger size cryogenic fuel stage and the also probably longer satellite related to a heavier payload enabled by better performing LOX-LH2 propulsion.

The SpaceLiner Orbiter reentry has been simulated with an entry interface speed of approximately 7.37 km/s . Reaching its once-around destination CSG in Kourou is without problem for the orbiter due to its still very good hypersonic L/D well above 2. The vehicle crosses Central America at high altitude and turns to the South over the Caribbean Sea reaching CSG from the Atlantic. Almost no sonic boom should be audible on ground. The maximum heatloads remain slightly lower than for the reference passenger concept because of a different AoA-profile and lower vehicle mass. The preliminary assumption of a common TPS with the passenger stage is confirmed by the reentry simulations.

2.7 Feasible point-to-point trajectories

Beyond the reference Australia – Europe and corresponding Europe – Australia missions, other alternative intercontinental connections have been studied since the beginning of SpaceLiner investigations. An early publication is reference 5 looking into different missions for SpaceLiner 2 and later with SpaceLiner 7 the trajectories and related constraints were becoming more and more refined (e.g. [2, 9, 10]). A systematic optimization of new point-to-point missions has been published in [24, 25]. In these references, trajectories of SpaceLiner 7 and SpaceX Starship have been analyzed regarding their overall feasibility. Many connections have been investigated for SpaceLiner 7 which are displayed on a world map in Figure 8. These all connect major economic, financial and population centers of the world. When avoiding flyover of large populated areas as best as possible, the layout of Earth has certain limitations regarding SpaceLiner flight routes. [24, 25]

These flight trajectories have been generated by using multi-objective optimization methods with evolutionary algorithms combining the ascent and descent phase of the flight. This methodology allows to minimize both important flight characteristics like the peak heat flux as well as the overall population that is overflowed. The latter is achieved by integrating the number of people living within the flight track using a worldwide population density database named GPWv4 [26]. Consequently, the optimizer aims to move the flights towards sparsely populated areas.

In general, the best areas for sparsely populated flight routes are bodies of water like the oceans. Additionally, the polar regions in the North and South are equally sparsely populated and offer the opportunity for large longitudinal crossings, for example from the Northern Atlantic to the Pacific Ocean.

In contrast, when flying over land the flight routes should avoid populated areas to mitigate the effect of sonic booms on the population which has been further investigated in [27]. This is of special concern in the northern hemisphere (Figure 9) which contains almost 90% of the population but only about two thirds of the land area. Furthermore, the land mass and the population living there extend into higher latitudes beyond 60 degrees while in the southern hemisphere most landmasses do not extend beyond 50 degrees latitude. As a consequence, it is far easier to connect the continents in the southern hemisphere by flying over the Antarctic region and the southern Oceans. Additionally, because the Indian Ocean extends from Antarctica to India itself, even people living on landmasses in the northern hemisphere can be served with these southern-oriented flight routes. [24, 25]

Because of the launch azimuth boundaries of the chosen launch sites, it has not always been possible to have a round trip connection. A round trip connection is understood as where the flight route can be served in both directions, like the reference mission Australia – Europe. In contrast, Australia – Florida, US is a one-way route as the flight goes around the polar region towards the East coast of the United States and Florida's launch heading range towards the east does not allow a launch back to Australia. Instead, in such a case the SpaceLiner vehicle could be imagined being part of a route system connecting multiple stops around the Earth. Here, this could for example be Australia – Florida – India – Australia as visible in Figure 8. If such multiple stops missions are attractive from the perspective of travel time saving is questionable. At least, such a connection option allows moving vehicles around the Earth and avoiding a dead end at certain commercially important locations.

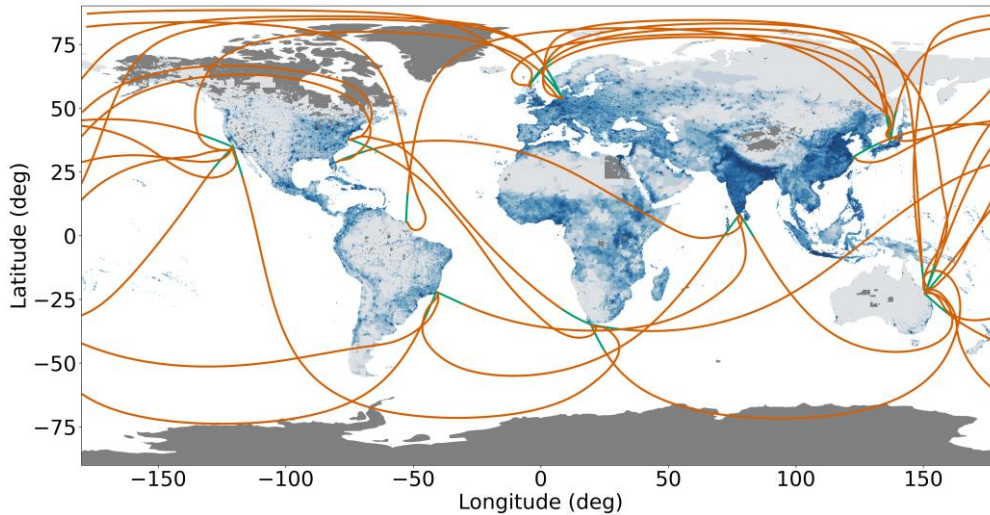


Figure 8: World map with computed potential SpaceLiner 7-3 trajectories (Green: Ascent, Orange: Descent) including population density, normalized between 1 (light-blue) and 1000 people/km² (dark-blue)

Beyond the heading range boundaries, the quality of a launch site in terms of surrounding land mass as well as location on the world map is a critical factor. The chosen location in Japan is adjacent to the Sea of Japan and only allows launching towards the North to the Arctic. Thereby, it can primarily be used to connect to Europe and the northern coast of South America. However, it is not suited to launch towards other launch sites in the Pacific, which might be a disadvantage regarding the available market share. This aspect shall be further investigated in the future.

aerothermal heatload environment requiring a new TPS. The redesign investigations of SpaceLiner 8 with dedicated focus on the upper or passenger stage (SLP) are trying to find a good compromise while keeping in mind feasible and attractive trajectories of a worldwide network. Results from an early systematic investigation are summarized in section 3.4.

3 PRE-DEFINITION OF SPACELINER 8 AND INTERMEDIATE STEPS

3.1 SL7 improvement potential

The biplane architecture of the mated launch configuration as shown in Figure 2 is not without problems because of complex high-speed flow interactions of the two stages during ascent flight. A 6DOF-simulation based on simplified aerodynamics assuming perturbations and engine-out conditions indicates that the situation could probably be mastered by TVC [11, 18, 28]. Nevertheless, a less interacting, less complicated flow around the geometry of the ascent vehicle is desirable not least to avoid potential damage to surface insulation and coatings.

Both, the complicated flow of the launch configuration and the shock-shock interaction during booster reentry [9, 18] have motivated the investigation of potential geometry changes and improvements to the SpaceLiner booster wing geometry. A refined model of the tank, its cryogenic insulation and external TPS with an overall increased thickness has an impact on the available volume for propellants inside the SLB which is to be addressed to keep the mission margins.

The integration of the passenger rescue system in the nose section of the upper stage and its reliable operation in all flight conditions is another critical aspect. Systematic analyses of the separation process with the SLP7 design have been performed in selected critical flight points [42, 43, 44]. A summary of these results is included in section 2.4 which shows need for a future redesign of the passenger capsule and its integration in the passenger stage.

In order to establish (an under realistic assumptions feasible) worldwide network of intercontinental point-to-point connections (see previous section 2.7), the aerodynamic shape of the winged upper stage should be adapted in a way that it not only allows the smooth reentry gliding of SpaceLiner 7 at good L/D



Figure 9: Potential SpaceLiner 7-3 trajectories viewed from above the North Pole

The assessments in [24, 25] are all based on the SpaceLiner 7 and its design constraints. Range cannot be extended beyond the capabilities of the maximum propellant loading listed in Table 7 or the vehicle's geometry would need to be changed. Only partial usage of propellant was assumed possible, although a more detailed evaluation of the tank system will be required. For some missions it could be attractive "jumping over" densely populated areas by partially flying outside of the atmosphere to eliminate any sonic boom reaching ground. However, such maneuvering is hardly possible with SpaceLiner 7 because of trim constraints and changes in the

but also in certain cases being capable of “jumping over” densely populated continental areas.

Currently, the study for the next SpaceLiner 8 design is ongoing and a consolidated configuration is not yet defined. However, design activities are intensifying and some key results which guide future developments are presented in the following subsections.

3.2 SLB8 with small fixed wing

In order to reduce biplane flow interactions during ascent and to avoid the shock-shock-interaction on the outboard leading edge, a drastically reduced size of the SLB wing had been investigated and a sketch of the concept was presented in [9]. The relatively small wing of the so called SLB8V2 turns out to be fully sufficient for a smooth reentry avoiding extreme heatloads. However, the SLB8V2 would need to be designed for vertical downrange landing on a sea-going ship. The reentry could be somehow similar to SpaceX’ Starship. After gliding deceleration to low speed and low altitude, the vehicle should rotate its attitude by 180 deg. and eventually some of the rocket engines are reignited for final slowing down to a vertical landing.

The turning maneuver of SLB8V2 before its intended vertical landing, as the procedure was assumed by DLR, has been described in [9]. The large propulsive moment required for a controlled pitch-turn maneuver was evaluated as a critical point for the feasibility of the concept [9].

Meanwhile, SpaceX has concluded several flight demonstrations with Starship prototypes at its Boca Chica site, Texas. Five subsequent test vehicles (SN8 - SN11 and SN15) were reaching at least 10000 m altitude in ascent flight before performing a controlled “sky-dive” maneuver at very low air-speed. The latter makes the major difference to the SLB8V2 assumption of aerodynamically controlled flight with dynamic pressure of at least 10 kPa. Simulations performed by DLR for the Starship returning from space [37] show that operational dynamic pressure would be rather in the range of 3 to 6 kPa, figures also supported by SpaceX’ announcement. Starship is controlling its attitude by changing the dihedral deflection of both canard and main wing before rapidly performing the “belly-flop”-maneuver which rapidly brings the vehicle from almost horizontal into vertical orientation for landing. The turn is simply achieved by folding-up the aft wing and hence eliminating lift and at low dynamic pressure the TVC of three reignited SpaceX Raptor-engines controls attitude and decelerates the falling stage. Similar maneuvers were hardly achievable with the previously defined SLB8V2 as described in [9].

Although, at least the final and successful SN15 flight test of Starship can be understood as a major breakthrough, the innovative “sky-dive”- and “belly-flop”-maneuvers are highly demanding for the wing design and its control as well as the fast rocket engine reignition. Therefore, suitability of this approach also for safe and efficient operation of the SpaceLiner booster is still open for future evaluations.

3.3 SLB8 option with swept wings

As the vertical landing SLB8V2 turned out to be not fully convincing, alternative designs have been explored [9, 11]. It has been tried to maintain the promising hypersonic aerodynamic configuration with small fixed wings, however, in order to allow the stage to use “in-air-capturing” [21, 22, 23] and horizontal landing, deployable wing options have been checked on

integration and mass impact [9, 11]. The challenge of this design is finding a suitable combination of different wing shapes which achieve a sufficiently high trimmed subsonic L/D of around 6, acceptable landing speed but also being fully trimable in hypersonic flight at high-angles of attack. A partially automatic variation of parameters was implemented in an MDA approach in order to systematically search for feasible and promising lay-outs shown in [11]. Instead of trailing edge flaps the inner segment had separate spoilers on its lower and upper surface.

A critical aspect for RLVs like the SpaceLiner is the selection of reusable cryogenic tank insulation which works under multiple environmental conditions. Independent of weather conditions (e.g. temperature, humidity) effective insulation needs to be ensured and icing on the vehicle external surface is to be avoided. DLR has performed systematic research on promising combinations of insulation and reentry TPS for which the SLB7-3 serves as the reference system concept. The booster stage’s reusable cryogenic tank insulation has been investigated under consideration of the external TPS by numerical simulation and experiments [34, 35, 36]. The pre-selected design option includes a so-called purge gap creating a distinct gap between the insulation of the cryogenic tank and the external thermal protection system, which has to be resistant to temperatures beyond typical limits of cryo-insulations. This relatively complex combination of external TPS and cryogenic insulation has been selected in order to avoid icing even in humid and relatively cold environment [34]. In the gap a forced flow of pre-heated dry gas is providing a controlled boundary condition at the outer interface of the cryogenic insulation. Results from the DLR projects AKIRA and TRANSIENT demonstrate the reusable insulation concept is functioning, however, a mass impact on the SLB stage is expected [35, 36]. This effect is due to the increased weight per surface area but also by the reduced available volume for propellants inside the SLB because of the enlarged thermal protection thickness compared to the previous assumptions.

At the end of the AKIRA-project such an influence on the reference system has been investigated using the SLB8V3-variant presented in [11]. Three iteration steps were performed (see short summary in [43]) considering the definition of the thermal protection system as well as cryogenic insulation based upon AKIRA-investigations. A TPS with external metallic surface (either Inconel or Titanium or Aluminum depending on the expected maximum temperatures) has been assumed.

In the final Iteration 3 of the SLB8 design it has been decided to add an additional, 10th rocket engine to improve thrust-to-weight ratio at lift-off, thus, reducing gravity losses with almost similar ascent propellant mass compared to SLB7-3. The outer dimensions of the SLB8V3 configuration in Iteration 3 are shown in Figure 10. The fuselage diameter is increased to 8.8 m. As a consequence, the stage length reduces to 79.1 m (without body flap). Aerodynamic performance requirements of the In-Air-Capturing method lead to an increased wing size. The wing is inclined by 2.5° with respect to the fuselage rotational axis. The overall span is at 53.8 m while the mid-chord length increases to 9.9 m. Higher masses for thermal protection, propulsion and structure changes the axial center of gravity position that is calculated at $x = 57.108$ m from the nose of the booster stage in case of the outer wing segment deployed. In case of folded outer wings, the center of gravity position is calculated at $x = 57.243$ m. [43]

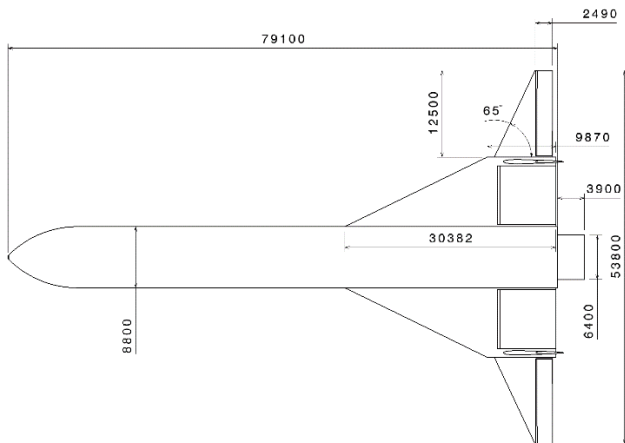


Figure 10: SLB8V3 Iteration 3 – dimensions, deployed outer wing segment [43]

Estimated dry mass of the SLB8V3 Iteration 3 reaches 220 Mg; slightly less than for the Iteration 2. However, its significantly lower GLOW makes Iteration 3 the more robust and more compact design. Despite these advantages, more analyses are needed to define the SpaceLiner 8 booster stage.

A recent systematic numerical assessment on the heatflux peaks originating from the shock-shock interaction show that these are probably less critical for the design of the outer wing leading edge than previously assumed [33] because the estimated nominal peak temperatures are excessively pessimistic. Further, trim capabilities of the large spoilers in hypersonic flow at high angles of attack are compromised by separated flowfields. If a design similar to the one shown in Figure 10 would be chosen, a dedicated study on the spoiler efficiency would have to be performed.

3.4 Multi-disciplinary design variations in preparation of SLP8

A systematic variation and assessment of potential design options is carried-out in a multi-disciplinary approach. The focus of the work is on finding an improved geometry for integration of the capsule and an extension of the feasible flight regime. In these analyses the outer shape of the fuselage, the internal arrangement of tanks and engines and the large vertical stabilizer are still kept similar to the SLP7. Future evolutions towards a consolidated SpaceLiner 8 configuration might be extended to modifications also on these items. Focus of the current variation is thus on the wing shape and planform while considering an improved capsule integration.

The shortcomings of the SpaceLiner 7 capsule design and of its stage integration have already been discussed in the previous section 2.4. As a first measure, the “Type C” integration (schematically shown in [43, 44]) is selected as baseline which should allow a simplified and faster separation process only in the forward direction (Figure 11). Further, the architecture is now split in three sections which should be easily separable. The core capsule segment is mostly similar to the previous SLC7, however, slightly shortened by about 1.5 m. The front pressure dome is the most forward point but no longer including the ablative TPS on the blunt nose. Instead a conical nose section (called LSCS) is reaching about 3.7 m to the nose and will be protected by TPS. The Liquid Separation & Control System (LSCS) comprises bi-propellant separation motors and the RCS of the stage. The new liquid separation motor is pulling the capsule in case of extreme emergencies and would reduce the number of solid separation motors at the

aft end of the capsule from five to four. The LSCS tank system should feed both RCS and separation motors and as this propellant is used in the nominal mission for attitude control and liquid separation motors having a better Isp than solids, a mass saving is expected. With the RCS moved forward the aft end of the core capsule could be shortened by roughly 1 m.

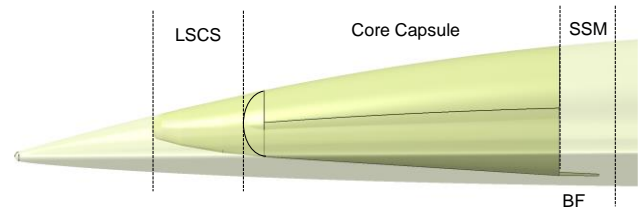


Figure 11: Potential SLP8 capsule integration concept

Behind the capsule the Solid Separation Motor (SSM) section is placed, still containing four of the solid motors as described in section 2.4 and which are shown in [43, 44]. However, the SSM is no longer directly connected with the SLC but serves structurally more the role of an interstage. This new connection should bring safety improvements as the solid motors usually remain connected with the propulsion system of SLP and only in case of extreme emergency push the SLC out of the danger zone. After a couple of seconds, the SSM should be separated and the capsule should be flying in a configuration as shown in Figure 12. After the potential reentry and most likely before parachute deployment, the LSCS will also be separated to simplify the landing of the capsule. The actual operational concept will be based on future detailed studies.

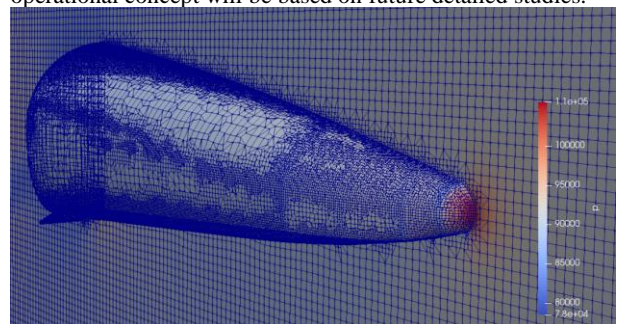


Figure 12: SLC8 aerodynamic shape with mesh

The aerodynamic concept as presented in Figure 12 is subject to ongoing investigations to improve the capsule’s stability characteristics. Engineering methods as well as CFD inviscid Euler calculations with the OpenFOAM environment and the compressible *rhoSimpleFoam* solver are used. The hex-dominant meshes are generated with the *snappyHexMesh* utility of OpenFOAM. The Mach distribution at a typical ground separation flight point of $M=0.5$, at altitude 1 km, AoA of 0° and body flap deflection of 20° is shown in Figure 13 and its velocity streamlines in Figure 14.

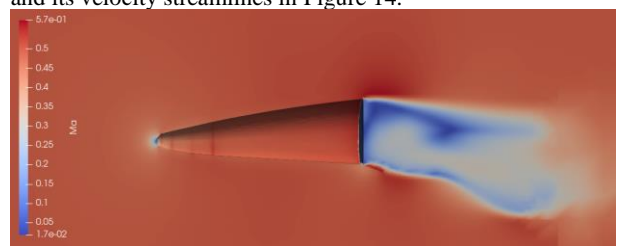


Figure 13: Mach distribution around potential SLC8

The aerodynamic and flight dynamic assessment in the complete flight regime is not yet sufficiently advanced that conclusive results are available. Therefore, the shape of the SLC8 as presented in Figure 12 through Figure 14 is preliminary and might see some adaptations.

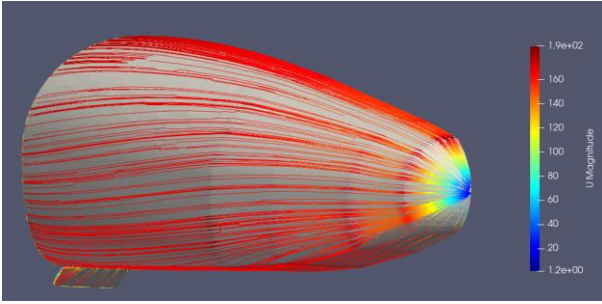


Figure 14: Velocity streamlines on potential SLC8

The passenger stage SLP8 design variations are based on the capsule predefinition. The challenge of the new stage design is to find an aerodynamic shape that allows both long-range glide missions with good hypersonic L/D, as in the case of SL7, and ballistic jumps outside the atmosphere over populated landmasses. For the latter, it is possible to eliminate all noise on the ground, but then the configuration's design needs to generate increased lift at increased AoA during re-entry to remain within acceptable heat loads. To address these somewhat contradictory requirements, a multidisciplinary design optimization methodology has been established. Based on fast estimation methods the geometry of the wings has been systematically varied with regard to maximum SLP hypersonic lift-to-drag ratio, maximum trimable hypersonic lift generation as well as the resulting dry mass of the vehicle.

For the optimization of both, the aerodynamic properties and the trajectories, Python wrappers were used to access the DLR legacy tools used for trajectory simulation, mass modelling and aerodynamic performance computation. A genetic multi-objective algorithm from the *pymoo* [45] library was used for both optimizations, specifically the NSGA-III algorithm [46, 47].

The shift of CoG induced by the wing geometry variation has been assessed in all cases and considered for the generation of pitch-pre-trimmed aerodynamic datasets. In addition, other constraints such as a maximal permissible landing speed of 100 m/s and a feasible flight path through the entire velocity regime were taken into account. Figure 15 shows as an example five potential shapes and the resulting characteristics in 4 dimensions.

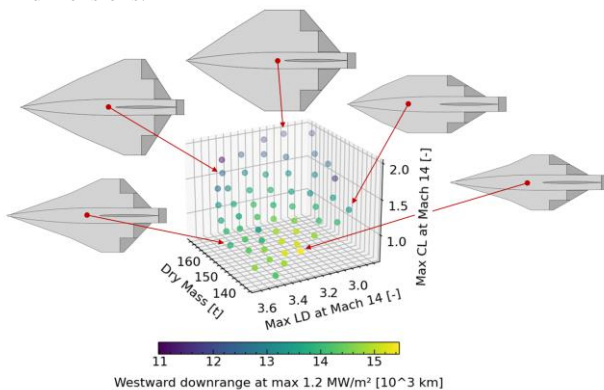


Figure 15: SLP8 design variants and resulting system characteristics

More than 20000 different SLP8 variants have been tried out by the automated MDA-algorithms and a huge number of plots have been generated similar to the example presented in Figure 16. Note the SpaceLiner 7 SLP highlighted as red cross for comparison. While its trimmed L/D in hypersonic is very good and can be hardly improved (as was exactly intended in the past, see [12, 13]), the dry weight of the stage is close to

the upper limit and its capability for generating high lift by increasing AoA is limited. The latter need is a driving factor in the definition of SLP8 while a weight approaching that of SLP7 would still be acceptable, it should not exceed it.

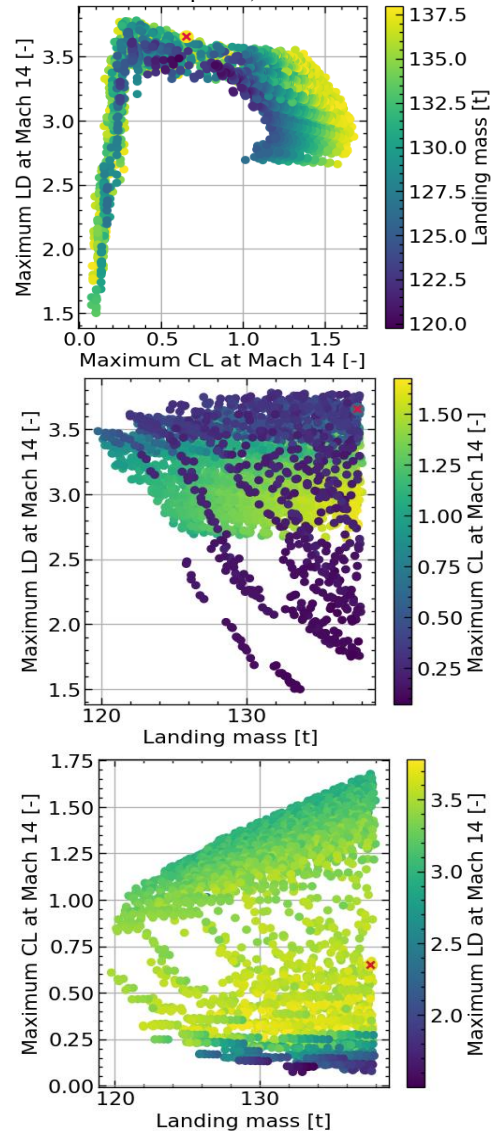


Figure 16: Typical results of systematic SLP8 design variations and impact on aerodynamic performance [48]

The process of parametric geometry variation and adaptation under several constraints (e.g. flap integration) and the generation of the related aerodynamic and performance characteristics are run fully automatic. Obtained data are post-processed and plotted similar to Figure 16. The pareto-fronts can be identified and analyzed by the stage designer to find promising design regions. These are further checked on robustness to some uncertainties, like CoG-position having a significant impact on vehicle trimability and hence achievable performance. The aerothermodynamic characteristics of all promising candidates are crosschecked with OpenFoam-CFD analyses and will be later subject to critical assessment of heatflux based on mission-optimized trajectories.

Some subsonic flow conditions of the SLP8 variant O40-0042 at Mach 0.5 and wing flap deflection of 10° are shown in Figure 17 and Figure 18. This specific configuration, currently evaluated as highly promising for SpaceLiner 8, shows remarkable similarities to the SLP7. However, the span is reduced and wing sweep angles are slightly adapted and as a consequence the generated lift is increased in hypersonics at

elevated trimable AoA. The sensitivity of the aerodynamic characteristics to modelling requires careful checks by CFD-(Euler-)methods before any configuration can be finally selected. In particular, the landing speed aerodynamics need to be considered to confirm practical feasibility of the potentially smaller size wing.

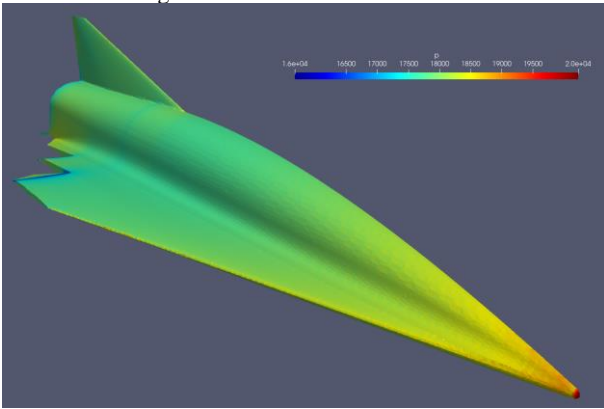


Figure 17: Pressure distribution on SLP8 variant O40-0042 at M=0.5, AoA=0°

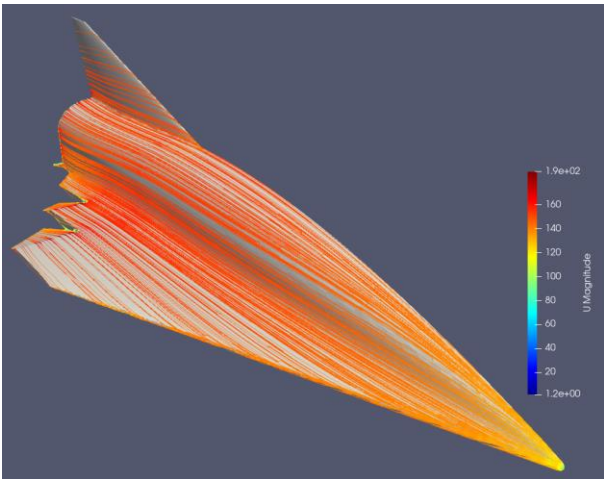


Figure 18: Velocity streamlines on SLP8 variant O40-0042 at M=0.5, AoA=0°

An essential step of the multi-disciplinary design process are trajectory optimizations similar to those described in section 2.7 to evaluate the mission performance of the most promising configurations. In the end, not the discrete aerodynamic characteristics are decisive but the optimized integral of all impact factors.

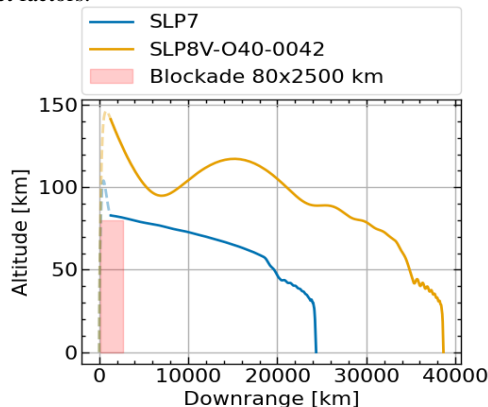


Figure 19: Potential downrange capability of SLP8 vs. SLP7 in generic “eastward” trajectories

Before the trajectory optimizations are applied to potential realistic point-to-point missions, generic trajectories launched

from the equator simply in eastward, northward, and westward direction are calculated, revealing already some concepts as less attractive. The example plot in Figure 19 compares the SpaceLiner 7 with the SLP8 variant O40-0042 for a theoretical purely eastward flight under the new constraint that after MECO the stage should stay above 80 km for a distance of at least 2500 km to eliminate the sonic boom in the overflown (potentially densely populated) area. Further, in this example the downrange is maximized. Based on the current status, the SLP8 shows potential for major improvement.

3.5 Intermediate development steps before SpaceLiner

The SpaceLiner defined as a fully-reusable, multiple-mission launch vehicle with advanced rocket engines requires mastering of ambitious technologies. The European expertise of today is limited to expendable launchers with cryogenic propulsion (Ariane 5 and 6). Directly starting the development of the SpaceLiner on such basis is risky, the more as it should also operate as a safe and commercially attractive passenger transport.

During several SpaceLiner Design Workshops potential development roadmaps have been discussed. Gaining expertise with a partially reusable space transportation system in flight operations as pure cargo carrier would be a major de-risking element before starting the commercial development of the SpaceLiner. An attractive option for such an RLV is a large reusable booster stage accelerating expendable upper stages which could be introduced as a successor to Ariane 6 after 2035.

DLR has started investigation of such launchers with the internal project name RLV-C4 [39, 40, 41]. A systematic variation of design options on propellant choice or aerodynamic configuration has been carried-out. One concept with the SLME as the main engine serves as RLV-reference in the FALCon-project [22, 23] and its architecture has some similarities to the SLB8V3 (Figure 10), however, with significantly reduced propellant loading (380 Mg) and only four SLME [40, 41].

Approaching or even exceeding the payload performance expected for Ariane 6 in GTO or Lunar exploration missions would require extremely tall launcher configurations in case of tandem-staged TSTO with reusable first stage. Therefore, for this class of RLV a parallel stage-arrangement is preferable: a winged stage is connected to an expendable upper segment with various internal architectures. References 39 to 41 have demonstrated that a payload of 14 tons into GTO with multiple payload capability can be achieved by a 3-stage architecture while still remaining at relatively compact size. Less demanding missions to different LEO can be served as TSTO.

The 2nd expendable stage is defined as an H150 and becomes even more compact than the core stage of the classical Ariane 5G. Note the expendable stage arrangement with the H150 forward skirt or 2-3-interstage adjacent to the RLV intertank ring (Figure 20 at left and center). The third launcher option investigated uses the same winged RLV first stage but merely a significantly smaller expendable upper stage to serve smaller payloads in low-energy missions. Figure 20 at right depicts a technical solution with the same attachment point on the RLV and the small H14 expendable upper stage of the 3STO powered by Vinci-engine and significantly reduced size of the payload fairing. Investigations show that despite significantly higher RLV-separation speeds of the Mini-TSTO compared to the heavier launcher variants on its left, the overall vehicle

lay-out can be maintained with the external TPS strengthened. [41]

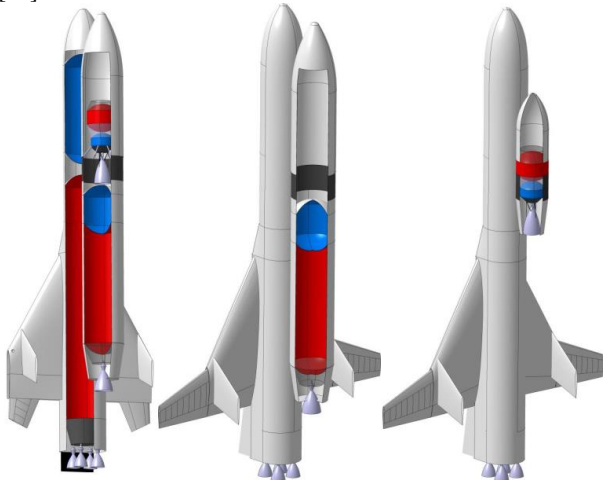


Figure 20: Launcher architecture sketches of RLVC4-B configuration as 3STO (left), TSTO (center) and Mini-TSTO (right) [41]

4 CONCLUSION

The DLR proposed reusable winged rocket SpaceLiner for very high-speed intercontinental passenger transport is progressing in its conceptual design phase after having successfully completed its Mission Requirements Review (MRR). Research on the vehicle is continuously performed with support from several EC-funded projects with numerous European partners. Assuming advanced but not exotic technologies, a vertically launched rocket powered two-stage space vehicle is able to transport about 50 passengers over distances of up to 17000 km in about 1.5 hours.

Systematic optimizations of point-to-point missions connecting major economic, financial and population centers of the world have been analyzed for SpaceLiner 7 and its design constraints regarding general feasibility. Unfortunately, for the feasibility of some attractive missions, “jumping over” densely populated areas by partially flying outside of the atmosphere to eliminate any sonic boom reaching ground is hardly possible with SpaceLiner 7 because of trim constraints.

The redesign investigations of SpaceLiner 8 are trying to find a good compromise for the upper or passenger stage (SLP) while keeping in mind feasible and attractive trajectories of a worldwide network. The passenger rescue capsule, designed to be used in cases of extreme emergencies, has to be also improved which is addressed in parallel with the SpaceLiner 8 redefinition. A new, preliminary integration concept of SLC8 is presented. Sophisticated, automated multi-disciplinary analyses help in finding the best compromise out of the many design choices in the definition of the upper stage. A refined modelling of the cryo-tank’s reusable insulation on the booster stage (SLB) led to an overall feasible and promising concept but also to an increase in dry weight of the stage. Adding one more SLME on the SLB is the preferred choice for version 8 which limits the overall growth of the SpaceLiner.

The SpaceLiner 8 definition is not yet completed but a technically and operationally promising approach is identified and major steps forward are evident.

5 ACKNOWLEDGEMENTS

The authors gratefully acknowledge the contributions of Ms. Carola Bauer, Ms. Mona Carlsen, Ms. Elena Casali, Ms. Nicole Garbers, Ms. Carina Ludwig, Ms. Sarah Lipp, Ms. Olga Trivailo, Ms. Cecilia Valluchi, Ms. Natascha Bonidis, Mr. Alexander Kopp, Mr. Ryoma Yamashiro, Mr. Sven Stappert, Mr. Tommaso Mauriello, Mr. Magni Johannsson, Mr. David Gerson, Mr. Jochen Bütünley, Mr. Sven Krummen, Mr. Tobias Schwanekamp, Mr. Marco Palli, Mr. Jan-René Haferkamp and Mr. David von Rüden to the analyses and preliminary design of the SpaceLiner.

6 REFERENCES

1. Musk, E.: Making Life Multi-Planetary, in *NEW SPACE*, VOL. 6, NO. 1, 2018, [doi: 10.1089/space.2018.29013.emu](https://doi.org/10.1089/space.2018.29013.emu)
2. Sippel, M.; Stappert, S.; Koch, A.: Assessment of Multiple Mission Reusable Launch Vehicles, IAC-18-D2.4.04, 2018, [Download Link](#)
3. Sippel, M., Klevanski, J., Steelant, J.: Comparative Study on Options for High-Speed Intercontinental Passenger Transports: Air-Breathing- vs. Rocket-Propelled, IAC-05-D2.4.09, October 2005
4. Sippel, M., Klevanski, J., van Foreest, A., Gülhan, A., Esser, B., Kuhn, M.: The SpaceLiner Concept and its Aerothermodynamic Challenges, 1st ARA-Days, Arcachon July 2006
5. Sippel, M., van Foreest, A.: Latest Progress in Research on the SpaceLiner High-Speed Passenger Transportation Concept, IAC-07-D2.7.07, September 2007
6. Sippel, M.: Promising roadmap alternatives for the SpaceLiner, *Acta Astronautica*, Vol. 66, Iss. 11-12, (2010)
7. Trivailo, O. et.al.: SpaceLiner Mission Requirements Document, SL-MR-SART-00001-1/2, Issue 1, Revision 2, SART TN-005/2016, 11.07.2016
8. Sippel, M.; Schwanekamp, T; Trivailo, O; Kopp, A; Bauer, C; Garbers, N.: SpaceLiner Technical Progress and Mission Definition, AIAA 2015-3582, 20th AIAA International Space Planes and Hypersonic Systems and Technologies Conference, Glasgow, July 2015, [Download Link](#)
9. Sippel, M.; Stappert, S.; Bussler, L.; Forbes-Spyratos, S.: Technical Progress of Multiple-Mission Reusable Launch Vehicle SpaceLiner, HiSST 2018-1580839, 1st HiSST: International Conference on High-Speed Vehicle Science Technology, Moscow, November 2018, [Download Link](#)
10. Sippel, M.; Stappert, S.; Koch, A.: Assessment of multiple mission reusable launch vehicles, in *Journal of Space Safety Engineering* 6 (2019) 165–180, <https://doi.org/10.1016/j.jsse.2019.09.001>
11. Sippel, M.; Stappert, S.; Bussler, L.; Singh, S.; Krummen, S.: Ultra-Fast Passenger Transport Options Enabled by Reusable Launch Vehicles, 1st FAR conference, Monopoli, September 30th – October, 3rd 2019, [Download Link](#)
12. Sippel, M.; Schwanekamp, T.: The SpaceLiner Hypersonic System – Aerothermodynamic Requirements and Design Process, 8th European Symposium on Aerothermodynamics for Space Vehicles, Lisbon, March 2015

13. Schwanekamp, T.; Bauer, C.; Kopp, A.: The Development of the SpaceLiner Concept and its Latest Progress, 4TH CSA-IAA CONFERENCE ON ADVANCED SPACE TECHNOLOGY, Shanghai, September 2011
14. Van Foreest, A., Sippel, M.; Gülhan, A.; Esser, B.; Ambrosius, B.A.C.; Sudmeijer, K.: Transpiration Cooling Using Liquid Water, Journal of Thermophysics and Heat Transfer, Vol. 23, No. 4, October–December 2009
15. Reimer, Th.; Kuhn, M.; Gülhan, A.; Esser, B.; Sippel, M.; van Foreest, A.: Transpiration Cooling Tests of Porous CMC in Hypersonic Flow, AIAA2011-2251, 17th International Space Planes and Hypersonic Systems and Technologies Conference, 2011
16. Schwanekamp, T.; Mayer, F.; Reimer, T.; Petkov, I.; Tröltzsch, A.; Siggel, M.: System Studies on Active Thermal Protection of a Hypersonic Suborbital Passenger Transport Vehicle, AIAA Aviation Conference, AIAA 2014-2372, Atlanta, June 2014
17. Sippel, M., Trivailo, O., Bussler, L., Lipp, S., Kaltenhäuser, S.; Molina, R.: Evolution of the SpaceLiner towards a Reusable TSTO-Launcher, IAC-16-D2.4.03, September 2016, [Download Link](#)
18. Sippel, M.; Bussler, L.; Kopp, A.; Krummen, S.; Valluchi, C.; Wilken, J.; Prévèreaud, Y.; Vérant, J.-L.; Laroche, E.; Sourgen, E.; Bonetti, D.: Advanced Simulations of Reusable Hypersonic Rocket-Powered Stages, AIAA 2017-2170, 21st AIAA International Space Planes and Hypersonic Systems and Technologies Conference, 6-9 March 2017, Xiamen, China, [Download Link](#)
19. Sippel, M., Wilken J.: Preliminary Component Definition of Reusable Staged-Combustion Rocket Engine, Space Propulsion 2018, Seville, May 2018, [Download Link](#)
20. Sippel, M.; Stappert, S.; Pastrokakis, V.; Barannik, V.; Maksiuta, D.; Moroz, L.: Systematic Studies on Reusable Staged-Combustion Rocket Engine SLME for European Applications, Space Propulsion 2022, Estoril, Portugal, May 2022, [Download Link](#)
21. Sippel, M.; Stappert, S.; Singh, S.: RLV-Return Mode “In-Air-Capturing” and Definition of its Development Roadmap, 9th European Conference for Aeronautics and Space Sciences (EUCASS), Lille, June 2022, [Download Link](#)
22. Sippel, M.; Singh, S.; Stappert, S.: Progress Summary of H2020-project FALCon, Aerospace Europe Conference 2023 – 10th EUCASS – 9th CEAS, Lausanne July 2023, [Download Link](#)
23. Singh, S.; Bussler, L.; Bergmann, K.; Sippel, M.: Mission Design and Sensitivity Analysis for In-Air Capturing of a Winged Reusable Launch Vehicle, IAC-23-D2.5.5, 74th International Astronautical Congress (IAC), Baku, Azerbaijan, 2-6 October 2023
24. Callsen, S.; Wilken, J.; Stappert, S.; Sippel, M.: Feasible options for point-to-point passenger transport with rocket propelled reusable launch vehicles, IAC-22-D2.4.7, 73rd International Astronautical Congress (IAC), Paris, September 2022
25. Callsen, S.; Wilken, J.; Stappert, S.; Sippel, M.: Feasible options for point-to-point passenger transport with rocket propelled reusable launch vehicles, Acta Astronautica 212 (2023) 100–110, <https://doi.org/10.1016/j.actaastro.2023.07.016>
26. Gridded Population of the World, Version 4 (GPWv4): Population Density, Palisades, NY: NASA Socioeconomic Data and Applications Center (SEDAC), Center for International Earth Science Information Network – CIESIN – Columbia University, 2016, <https://doi.org/10.7927/H4NP22DQ> accessed August 2023
27. Callsen, S.; Wilken, J.; Sippel, M.: Analysis of Sonic Boom Propagation and Population Disturbance of Hypersonic Vehicle Trajectories, 1st Aerospace Europe Conference – 10th EUCASS – 9th CEAS, Lausanne, Switzerland, 2023, [Download Link](#)
28. Krummen, S.; Sippel, M.: EFFECTS OF THE ROTATIONAL VEHICLE DYNAMICS ON THE ASCENT FLIGHT TRAJECTORY OF THE SPACELINER CONCEPT, CEAS Space Journal, Vol. 11, Nov. 2019, pp. 161–172, <https://doi.org/10.1007/s12567-018-0223-7>
29. Valluchi, C.; Sippel, M.: Hypersonic Morphing for the SpaceLiner Cabin Escape System, 7th European Conference for Aeronautics and Space Sciences (EUCASS), Milan 2017
30. Stappert, S.; Sippel, M.; Bussler, L.; Wilken, J.; Krummen, S.: SpaceLiner Cabin Escape System Design and Simulation of Emergency Separation from its Winged Stage, AIAA 2018-5255, 22nd AIAA International Space Planes and Hypersonic Systems and Technologies Conference, 17-19 September 2018, Orlando, Florida, USA
31. Bauer, C.; Kopp, A.; Schwanekamp, T.; Clark, V.; Garbers, N.: Passenger Capsule for the SpaceLiner, DLRK-paper, Augsburg 2014
32. Wilken, J.: SpaceLiner System Specification Document, SL-SS-SART-00026-1/1, SART TN-003/2018
33. Bussler, L.; Karl, S.; Sippel, M.: Shock-Shock Interference Analysis for SpaceLiner Booster, 2nd HiSST: International Conference on High-Speed Vehicle Science Technology, Bruges, September 2022
34. Sippel, M. et al: Enhancing Critical RLV-technologies: Testing Reusable Cryo-Tank Insulations, IAC-19-D2.5.10, 70th International Astronautical Congress, Washington 2019, [Download Link](#)
35. Wilken, J. et al: Testing combined cryogenic insulation and thermal protection systems for reusable stages, IAC-21-D2.5.4, Dubai 2021, [Download Link](#)
36. Reimer, T.; Rauh, C.; Di Martino, G.D.; Sippel, M.: Thermal Investigation of a Purged Insulation System for a Reusable Cryogenic Tank, Journal of Spacecraft and Rockets, 59 (4), p. 1205-1213, <https://doi.org/10.2514/1.A35252>
37. Wilken, J.; et al: Critical Analysis of SpaceX’s Next Generation Space Transportation System: Starship and Super Heavy, 2nd HiSST: International Conference on High-Speed Vehicle Science Technology, Bruges, September 2022, [Download Link](#)
38. Bussler, L.; Sippel, M.; von Rügen, D.F.: Reference Concept SLB 8 Booster, AKIRA report R-2004, SART TN-001/2020, March 2020
39. Sippel, M.; Stappert, S.; Callsen, S.; Dietlein, I.; Bergmann, K.; Gülhan, A.; Marquardt, P.; Lassmann, J.; Hagemann, G.; Froebel, L.; Wolf, M.; Plebuch, A.: A viable and sustainable European path into space – for cargo and astronauts, IAC-21-D2.4.4, 72nd International Astronautical Congress (IAC), Dubai, 25-29 October 2021, [Download Link](#)
40. Stappert, S., Sippel, M., Callsen, S., Bussler, L.: Concept 4: A Reusable Heavy-Lift Winged Launch Vehicle using the In-Air-Capturing method, 2nd HiSST: International

Conference on High-Speed Vehicle Science Technology, September 2022, Bruges, Belgium

41. Sippel, M.; Stappert, S.; Callsen, S.; Bergmann, K.; Dietlein, I.; Bussler, L.: Family of Launchers Approach vs. “Big-Size-Fits-All”. 73rd International Astronautical Congress (IAC 2022), 18-22 September 2022, Paris, France, [Download Link](#)
42. Bayrak, Y.M.: Multi-body Simulation of the SpaceLiner Cabin Rescue System, SART TN-009/2019, October 2019
43. Sippel, M., Stappert, S., Bayrak, Y.M.; Bussler, L., Callsen, S.: Systematic Assessment of SpaceLiner Passenger Cabin Emergency Separation Using Multi-Body Simulations, 2nd HiSST-conference, Bruges, September 2022
44. Sippel, M., Stappert, S., Bayrak, Y.M.; Bussler, L.: Systematic Assessment of SpaceLiner Passenger Cabin Emergency Separation Using Multi-Body Simulations, CEAS Space Journal, published online: 02 June 2023, <https://doi.org/10.1007/s12567-023-00505-z>
45. Blank, J.; Deb, K: pymoo: Multi-Objective Optimization in Python, in IEEE Access, vol. 8, pp. 89497-89509, 2020, [doi: 10.1109/ACCESS.2020.2990567](https://doi.org/10.1109/ACCESS.2020.2990567)
46. Deb, K.; Jain, H.: An evolutionary many-objective optimization algorithm using reference-point-based nondominated sorting approach, Part I: solving problems with box constraints, IEEE Transactions on Evolutionary Computation, 18(4):577–601, 2014, [doi:10.1109/TEVC.2013.2281535](https://doi.org/10.1109/TEVC.2013.2281535)
47. Jain, H.; Deb, K.: An evolutionary many-objective optimization algorithm using reference-point based nondominated sorting approach, Part II: handling constraints and extending to an adaptive approach. IEEE Transactions on Evolutionary Computation, 18(4):602–622, August 2014
48. Mauriello, T.: Multidisciplinary Design Analysis & Optimization of the SpaceLiner Passenger Stage, SART TN-014/2023, to be published December 2023

Further updated information concerning the SART space transportation concepts is available at:

<http://www.dlr.de/SART>